



Hydrophobization of fully bio-based epoxy polymers using water as solvent: Effect of additives

Daniel Angel Bellido-Aguilar^a, Shunli Zheng^a, Yinjuan Huang^a, Ye Sun^a, Xianting Zeng^b, Qichun Zhang^a, Zhong Chen^{a,*}

^a School of Materials Science and Engineering, Nanyang Technological University, 50 Nanyang Avenue, 639798, Singapore

^b Singapore Institute of Manufacturing Technology, 2 Fusionopolis Way, 138634, Singapore

ARTICLE INFO

Keywords:

Bio-based polymers
Hexanoic acid
Resveratrol
Cardanol
Hydrophobicity

ABSTRACT

Current epoxy industry still has a strong dependency on fossil-derived precursors as demonstrated in the use of bisphenol A-based resins. To improve the sustainability of the epoxy industry, bio-based chemicals have been explored for the synthesis of environmentally-friendly epoxy polymers. This paper reports the hydrophobization of fully bio-based epoxy coatings using only water as solvent. Three bio-based additives (hexanoic acid, resveratrol, and a cardanol-based epoxy resin) were studied aiming to enhance the hydrophobicity of the coatings. The curing reaction mechanisms have been extensively explored. The modified coatings showed better hydrophobicity, however, they tend to possess a lower crosslink density because these additives have, to some extent, disrupted the polymer network formation. The anticorrosion performance of the bio-based coatings was also evaluated and discussed based on the reported hydrophobicity and crosslink density. This study lays a foundation towards fully bio-based, environmentally-friendly polymers for hydrophobic applications in the future.

1. Introduction

The interest to use biomass-based compounds for the preparation of polymers has increased rapidly in recent years due to growing demand towards sustainability and environmental protection [1]. Traditional polymers are mostly derived from non-renewable fossil source [2], therefore, much effort is needed to design new polymers from bio-based compounds.

To date, fossil-based compound bisphenol A (BPA) continues to be the dominant raw material for the preparation of epoxy resins [3,4]. On the other hand, great effort has been made to synthesize bio-based epoxy resins from various sources such as lignin [5], vegetable oils [6], cellulose [7] and terpenoid [8]. However, development of full bio-based polymers remains a great challenge. Ideally, not only the epoxy resin should come from bio-sources, but also the other reagents in the overall formulation. This is particularly true when hydrophobicity is required in a number of applications.

In this research, new polymers were prepared in which the epoxy resin, curing agent and the hydrophobic additives were all derived from biomass. The bio-based thermoset used in this study was prepared from the epoxy resin diglycidyl ether of glycerol (GDE) and the curing agent was citric acid (CA). To the best of our knowledge, this bio-based epoxy

formula has not been reported in literature [4,9–12]. GDE and CA have been used separately in different epoxy formulae. GDE is a bifunctional epoxy resin that can be obtained from glycerol, which is a byproduct of the biodiesel industry [13–15]. However, the bio-based content of GDE can be negatively affected by type of epichlorohydrin used. Although epichlorohydrin can be obtained from bio-based glycerol, it is still mostly produced from non-renewable sources. Nevertheless, GDE is still an attractive bio-based chemical used in the synthesis of thermosets [16–23]. CA is a tricarboxylic acid that can be industrially prepared from sugar or from food and agricultural waste [24]. Although CA, as a curing agent, suffers from the inconvenience of being a solid at normal conditions, it has been used as a bio-based curing agent in the synthesis of epoxy coatings [25–27]. Due to their molecular structures, thermosets prepared by GDE and CA are hydrophilic. Therefore, hydrophobic additives have to be added to improve the hydrophobicity when water repellency is required.

Hydrophobic materials are well known for their ability to repel water that makes them potential candidates for a series of applications such as easy cleaning, anti-icing, and anticorrosion [28,29]. To improve the anticorrosion performance of polymers derived from GDE and CA, bio-based hydrophobic additives have to be incorporated. Potential candidates for bio-based hydrophobizers include hexanoic acid (HA),

* Corresponding author: School of Materials Science and Engineering, Nanyang Technological University, 50 Nanyang Avenue, 639798, Singapore.

E-mail address: ASZChen@ntu.edu.sg (Z. Chen).

<https://doi.org/10.1016/j.eurpolymj.2020.110043>

Received 30 April 2020; Received in revised form 17 September 2020; Accepted 18 September 2020

Available online 25 September 2020

0014-3057/ © 2020 Elsevier Ltd. All rights reserved.

trans-resveratrol (RV), and a bio-based resin NC-514S. HA or caproic acid is an aliphatic carboxylic acid that can be obtained from certain oils and from the fats of animals [30,31]. Although HA has been used as pendent chains in the preparation of the branched polymers [32], no reports have been found for its use as an additive in the synthesis of epoxy thermoset. HA is expected to impart some degree of hydrophobicity due to its aliphatic chain. RV is a polyphenol that can be extracted from grapes and peanuts [33–35]. The use of RV in the preparation of thermosets is scarce [36–39]. Due to its low water solubility (0.05 mg/mL) [40], RV may confer better hydrophobicity on GDE-CA polymers. Finally, NC-514S is epoxy resin derived from cardanol which is obtained from the cashew nutshell. NC-514S has been used in the preparation of bio-based thermosets [41–43] or composites [44,45]. NC-514S was selected as a potential bio-based hydrophobizer in the current study since a thermoset derived from NC-514S was proven to be hydrophobic [46].

2. Experimental section

2.1. Materials

Glycerol diglycidyl ether (technical grade) (GDE), citric acid (CA) and hexanoic acid (HA) ($\geq 98\%$) were purchased from Sigma Aldrich. The epoxy resin NC-514S (abbreviated as NC) was obtained from Cardolite. *Trans*-resveratrol (98%) (RV) was purchased from S1-Lab (Singapore). The molecular structures of the chemical used are shown in Fig. 1.

2.2. Synthesis of the bio-based polymer coatings

This research focuses on studying the accumulative effect of potential bio-based hydrophobizers (HA, RV and NC) on a basic epoxy formulation made of GDE and CA. Therefore, five different formulae were developed: two unmodified formulae (GDE-CA-0.90, GDE-CA-0.73) and three modified formulae (GDE-CA-HA, GDE-CA-HA-RV, and GDE-CA-HA-RV-NC) (Table 1). The three modified formulae were developed in order to understand how the accumulative incorporation of bio-based additives influenced on the hydrophobicity of the polymers.

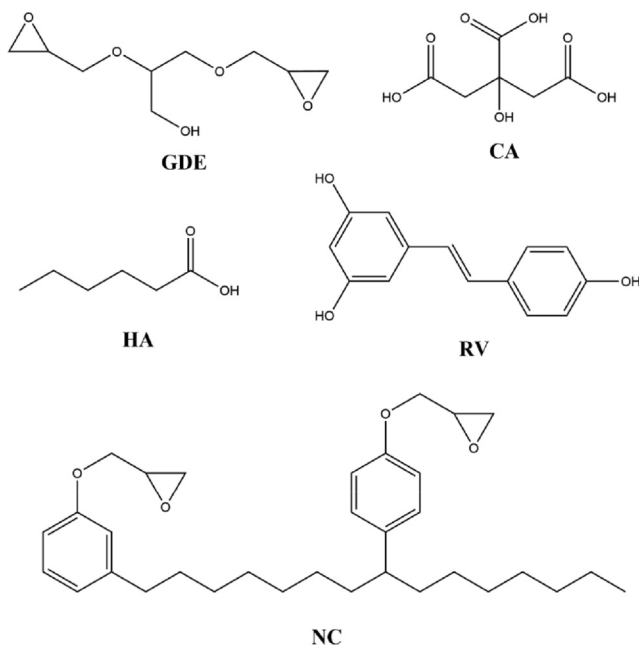


Fig. 1. Molecular structure of the bio-based compounds used in this research: GDE (glycerol diglycidyl ether), CA (citric acid), HA (hexanoic acid), RV (resveratrol) and NC (a cardanol-based resin).

Table 1

Composition of the five epoxy resin formulae.

Sample	Molar ratio of epoxy groups (GDE) to carboxylic groups (CA)	Bio-based additives (% w/w) with respect to GDE		
		HA	RV	NC
GDE-CA-0.90	1:0.9	–	–	–
GDE-CA-0.73	1:0.73	–	–	–
GDE-CA-HA	1:0.73	15	–	–
GDE-CA-HA-RV	1:0.73	15	9	–
GDE-CA-HA-RV-NC	1:0.73	15	9	1

The amount of bio-based additives, HA, RV, and NC used in relation with GDE was 15%, 9% and 1% w/w, respectively. The concentrations of these bio-based additives were carefully selected after investigating formulae with different concentrations of the bio-based additives. At these specific concentrations, hydrophobic effect was achieved on the basic formula of GDE and CA.

The molar ratio of epoxy groups of GDE to the carboxylic groups of CA was 1:0.9 for GDE-CA-0.90 and 1:0.73 for the other four formulae. Samples with molar ratios of GDE and CA higher than 1:0.9 were not included in this research as the coatings were produced with various surface defects. In addition, only the bio-based polymers with molar ratio 1:0.73 (GDE : CA) were modified because at this ratio the bio-based additives could be mixed homogeneously without any physical segregation.

The preparation of the unmodified formulae (GDE-CA-0.9 and GDE-CA-0.73) was done as follows. First, CA was dissolved in water in a mass ratio of 1:1. The CA solution was then heated at 120 °C in an oil bath under agitation for 10 min to remove around half of its water content to enable a good quality coating in the subsequent process. Afterwards, the hot CA solution was taken out of the oil bath and GDE was added and mixed for about 10 min.

For the preparation of the modified formulae (GDE-CA-HA, GDE-CA-HA-RV and GDE-CA-HA-RV-NC), the procedure to prepare the CA solution was the same as described above. In preparing GDE-CA-HA, HA and GDE were mixed first before being mixed with the CA. However, in the preparation of GDE-CA-HA-RV and GDE-CA-HA-RV-NC, GDE was initially mixed with RV (or RV and NC) and heated to 120 °C for about 10 min under constant stirring. Thereafter, the mixture was cooled down at ambient condition and mixed with HA. The reason for such processing procedure will be further explained later.

The final mixture was then poured on PTFE molds and stainless steel substrates (0.25 mm thick). The coatings were cured at 150 °C for 2 h with a heating and cooling rate of 0.5 °C/min, comprising around 10 h for the curing cycle. The slow heating and cooling rate was chosen in order to prevent the formation of surface defects on the coatings. The films prepared on the stainless steel substrates were used for the measurements of the wettability and corrosion tests. The samples prepared in PTFE molds were used for the rest of the characterizations. All the samples were analyzed immediately after their preparation.

2.3. Characterization

The epoxy equivalent weight (EEW) of the resins was obtained according to the standard titration method described in ASTM D1652. Two to four measurements were performed for each sample conditions.

Thermogravimetric analysis (TGA) was performed in a TGA Q500 (TA Instruments). Samples of about 8–12 mg were heated from room temperature to 600 °C at 10 °C/min under nitrogen flow (60 mL/min). Three measurements were conducted for each sample.

Differential scanning calorimetry (DSC) was carried out in a DSC Discovery (TA Instruments). The solid samples with the weight of around 7–11 mg were prepared in aluminum pans and heated three

times sequentially from -70 to 200 °C at 10 °C/min under nitrogen flow (50 mL/min). In order to remove the thermal history of the samples, the data of the last heating was used for the analysis. Three to five measurements were carried out for each formulation. For the reactivity tests, liquid samples with the weight around of 1 – 4 mg were prepared in hermetic aluminum pans and heated from 25 to 250 °C at four different heating rates (5 , 10 , 15 and 20 °C/min). In this experiment, the reported temperature is an average of two measurements.

The viscosity of the preheated samples was measured on a rheometer Discovery HR-3 (TA Instruments) configured in a parallel-plate geometry with a 500 - μ m gap at 25 °C.

Fourier-transform infrared (FTIR) spectroscopy was performed in a FTIR MIR/NIR Frontier (Perkin Elmer) in an attenuated total reflectance (ATR) mode for all the samples except for HA which was done in transmission mode using KBr pellets. The wavelength range of the analyses was 4000 – 600 cm^{-1} with a resolution of 4 cm^{-1} and 32 scan accumulations. A baseline correction was done in all the spectra using the software Spectrum (PerkinElmer).

The wettability of coatings was assessed in an OCA 20 goniometer (Dataphysics) by measuring the static contact angles of 5 μ L droplets of three different liquids (DI water, glycerol and ethylene glycol). The surface energy was calculated using the OWRK methodology [47–49] using the software SCA 20 (Dataphysics).

Dynamic mechanical analysis (DMA) was carried out in a DMA Q800 (TA Instruments) in a single cantilever mode with a deformation amplitude of 15 μ m at 1 Hz. The samples, prepared in rectangular shapes (35 mm in length, 14.3 mm in width, and 2.6 – 3.6 mm in thickness), were heated from -20 to 110 °C at a rate of 3 °C/min. At least three measurements were performed for each sample.

Hydrogen nuclear magnetic resonance (^1H NMR) spectroscopy was carried out on a Bruker Advance 300 NMR spectrometer with tetramethylsilane as the internal reference and chloroform- d (CDCl_3) and dimethyl sulfoxide- d_6 ($\text{DMSO-}d_6$) as solvents under ambient temperature. CDCl_3 was used only for the sample NC while $\text{DMSO-}d_6$ was employed for the rest of the samples. NMR data were collected via chemical shift (ppm, CDCl_3 and $\text{DMSO-}d_6$ resonance as the internal standard), multiplicity and integration.

Fresh samples with rectangular shapes, similar to those prepared for DMA, were soaked in DI water for water uptake measurements. The weights of the samples were measured using an analytical balance before being soaked and daily during the water immersion test until a water uptake equilibrium was achieved. The water uptake was reported as the percentage increase with respect to the dry sample.

The anti-corrosion performance of the coatings was analyzed in an electrochemical workstation (CHI 660d, Shanghai Chenhua Instrument Corporation). The measurements were carried out in a 3.5% w/w NaCl solution with Ag/AgCl and Pt as the reference and counter electrodes, respectively. Coatings with an exposed area of 1 cm^2 were soaked in the electrolyte for 7 days before the electrochemical analysis. At least three samples of each formulation were analyzed together with measurements of their thicknesses by using a conventional digital micrometer.

3. Results and discussion

3.1. Curing of coatings

The EEW of GDE was 146 g/eq and the presence of the epoxy groups was confirmed by the absorbance bands at 1254 cm^{-1} and 907 cm^{-1} that are related to epoxy ring vibrations [20,50] (Fig. 2). These epoxy bands were not present in the spectrum of the bio-based coatings, which would suggest a complete curing. However, a detailed inspection of the spectrum showed that the epoxy bands could be overlapped by other absorbance bands at the same wavenumber of the curing agent and precursors. Therefore, it was not possible to measure the degree of curing because of this overlapping. As it will be shown later, DSC was employed to determine whether the curing reaction was complete or

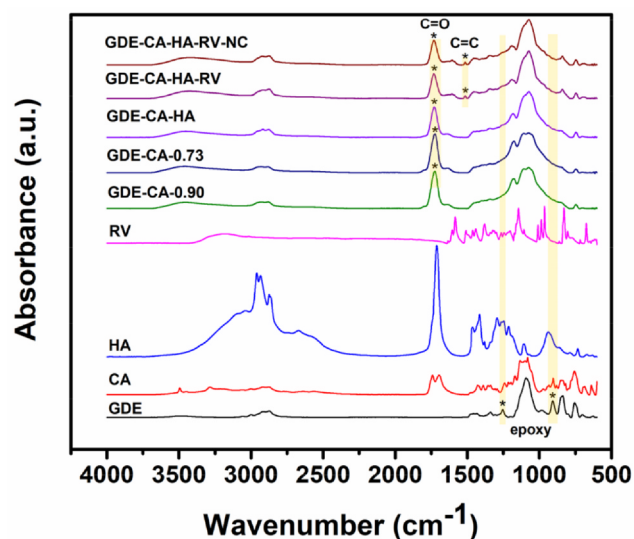


Fig. 2. FTIR spectra of the bio-based precursors (GDE, CA, HA and RV) and the bio-based coatings.

not. In relation with the spectrum of the bio-based coatings, all the samples had a characteristic band at around 1727 cm^{-1} that was attributed to the carbonyl group originated mainly from the presence of the curing agent CA [26]. In addition, samples containing RV showed a small absorbance band at around 1515 cm^{-1} , which was ascribed to the aromatic $\text{C} = \text{C}$ bond of RV [51].

To determine whether there was an unreacted compound within the GDE coatings, DSC was performed as shown in Fig. 3. The DSC curves only exhibited a glass transition point without trace of unreacted GDE. Therefore, we consider all the bio-based coatings were cured completely. Finally, it is worth mentioning that samples tend to plasticize when stored in humid conditions. A typical DSC curve of a plasticized polymer usually displays a lower glass transition and an endothermic process related to water desorption [52].

The reactivity of the curing reactions was analyzed by heating the samples at different heating rates. Fig. 4 shows typical DSC curves of the bio-based formulae. The curve displayed two characteristic peaks, one exothermic at the beginning of the heating and one endothermic at the end. In addition, some small endothermic peaks also occurred before the broad endothermic process. The exothermic process always

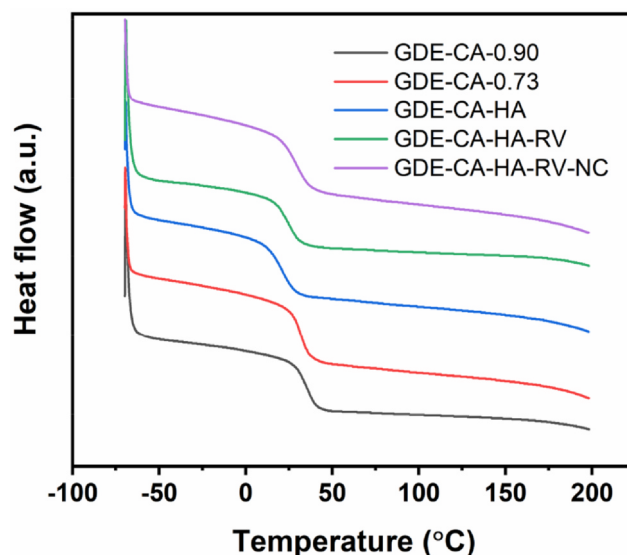


Fig. 3. DSC curves of the solid bio-based samples.

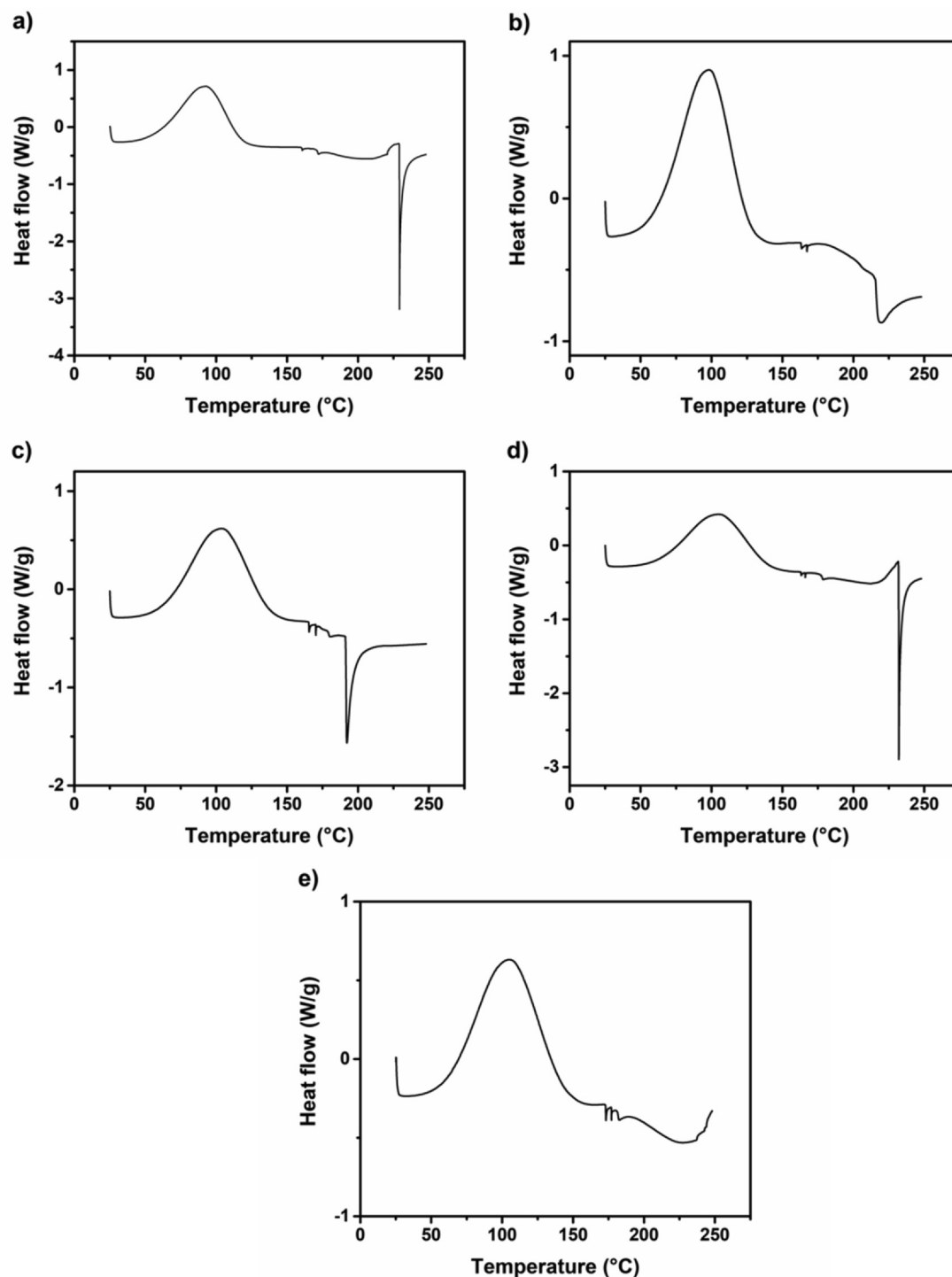


Fig. 4. Typical DSC profiles of the liquid bio-based formulae: (a) GDE-CA-0.90, (b) GDE-CA-0.73, (c) GDE-CA-HA, (d) GDE-CA-HA-RV and e) GDE-CA-HA-RV-NC.

occurred in the beginning of the heating while the intensity, width and position of the endothermic processes varied randomly. Therefore, due to its consistent presence, we believe that the exothermic peak is associated with the reaction between the epoxy groups of GDE and the carboxyl groups of the bio-based acid CA and HA. The small endothermic peaks may be the result of the secondary reactions whereas the broader endothermic peak is related to the water desorption prior to the polymer decomposition.

The reactivity of the main exothermic peak was studied by calculating the temperature at the maximum heat flow (T_{max}) for different heating rates (Table 2). The results clearly showed a common trend in

the T_{max} for all the heating rates. The lowest T_{max} was found in GDE-CA-0.90, followed by GDE-CA-0.73. The T_{max} continued to increase when HA was included. The T_{max} was similar among formulae containing HA (GDE-CA-HA, GDE-CA-HA-RV, and GDE-CA-HA-RV-NC).

The reaction of GDE and CA was more favorable when the concentration of the curing agent CA was higher. This suggests that CA is not only acting as a curing agent but also as a catalyst. That is, an autocatalytic reaction seemed to have occurred in the reaction of epoxy-carboxyl reaction caused by CA. However, the sole inclusion of HA (GDE-CA-HA) decreased the overall reactivity of the epoxy-carboxyl reaction as shown by the higher T_{max} . A possible explanation for this

Table 2

Temperatures ($^{\circ}\text{C}$) at the maximum heat flow (T_{max}) of the exothermic peak at different heating rates (values in parentheses represent the standard deviation).

Sample	T_{max} @5 $^{\circ}\text{C}/\text{min}$	T_{max} @10 $^{\circ}\text{C}/\text{min}$	T_{max} @15 $^{\circ}\text{C}/\text{min}$	T_{max} @20 $^{\circ}\text{C}/\text{min}$
GDE-CA-0.90	83.3 (± 0.6)	93.6 (± 0.8)	99.8 (± 0.9)	104.1 (± 0.9)
GDE-CA-0.73	88.1 (± 0.9)	99.1 (± 1.1)	105.0 (± 0.8)	109.4 (± 1.1)
GDE-CA-HA	94.0 (± 0.2)	105.0 (± 1.6)	111.4 (± 1.1)	116.6 (± 1.8)
GDE-CA-HA-RV	92.2 (± 1.2)	104.0 (± 2.1)	112.5 (± 0.5)	116.3 (± 2.2)
GDE-CA-HA-RV-NC	94.1 (± 1.9)	106.1 (± 1.0)	113.6 (± 1.0)	118.5 (± 1.8)

result is that certain concentration of HA may have reacted with GDE which has caused an increase in the T_{max} . HA is expected to be less reactive towards GDE than CA because of its lower acidity. The acidity of the first two deprotonations of CA ($\text{pK}_{\text{a}1} = 3.14$, $\text{pK}_{\text{a}2} = 4.76$, $\text{pK}_{\text{a}3} = 6.39$) [53] are higher than that of HA ($\text{pK}_{\text{a}} = 4.83$) [54]. Therefore, due to its lower acidity, HA was expected to react with GDE at a higher temperature than CA. Thus, the higher T_{max} observed in GDE-CA-HA can be ascribed to the effect caused by the reaction of HA with GDE. In summary, these results suggest that in GDE-CA-HA both CA and HA are simultaneously reacting with GDE.

The subsequent incorporation of RV and NC did not change the T_{max} , which suggests that neither RV nor NC has taken part in any epoxy group reaction in the DSC experiment. Therefore, the exothermic processes of GDE-CA-HA-RV and GDE-CA-HA-RV-NC were still attributed to the main reaction of GDE with CA and HA with no participation of RV and NC under these experimental conditions. Further discussion will be made next on how RV is incorporated into the polymer network.

3.2. Characterization of GDE-RV and GDE-RV-NC

In order to understand how RV and RV/NC were incorporated into the polymer network, it is important to recall the methodology to prepare GDE-CA-HA-RV and GDE-CA-HA-RV-NC. As described in the experimental section, GDE was first mixed and heated with RV or RV/NC before being mixed with CA and HA. The purpose of this experimental step was to allow the solid RV to be dissolved in GDE first so that a liquid mixture is formed that will allow the further addition of the other liquid compounds. The mixture GDE-RV and GDE-RV-NC was analyzed by NMR as shown in Fig. 5 a, b and compared with the spectra of GDE, RV and NC in Fig. 6. It can clearly be seen that the spectrum of GDE + RV is just a simple overlay by those of GDE and RV. In the spectrum of GDE-RV, the peaks from 6.0 ppm to 10.0 ppm are from RV, while those lower than 6.0 ppm correspond to GDE. Similarly, the spectrum of GDE-RV-NC is almost the same as that of GDE-RV (Fig. 5c). In addition, no characteristic peaks of NC were found in the spectrum of GDE-RV-NC. This can be explained by the low concentration of NC (1% w/w), which has made it hardly detectable.

Other characterizations were also performed for GDE-RV and GDE-RV-NC. The titration results showed that EEWs of GDE-RV and GDE-RV-NC were 181 and 191 g/eq, respectively. Therefore, the EEWs of GDE-RV and GDE-RV-NC were similar to each other but higher than that of GDE (146 g/eq). The higher EEWs of GDE-RV and GDE-RV-NC were attributed to the dilution effect caused by the incorporation of RV and RV/NC. Moreover, the viscosities of GDE, GDE-RV and GDE-RV-NC were 1.33P, 4.17P and 4.33P, respectively. Thus, the higher viscosities of GDE-RV and GDE-RV-NC (than GDE) were also ascribed to the presence of the bio-based additives RV and NC. To further assist the analysis, DSC profiles of GDE, GDE-RV and GDE-RV-NC were also obtained from -90 $^{\circ}\text{C}$ to 300 $^{\circ}\text{C}$, as shown in Fig. 7a. The DSC profile of GDE showed a characteristic glass transition at -67 $^{\circ}\text{C}$ and exothermic process around 150 $^{\circ}\text{C}$. The glass transition exhibited by GDE

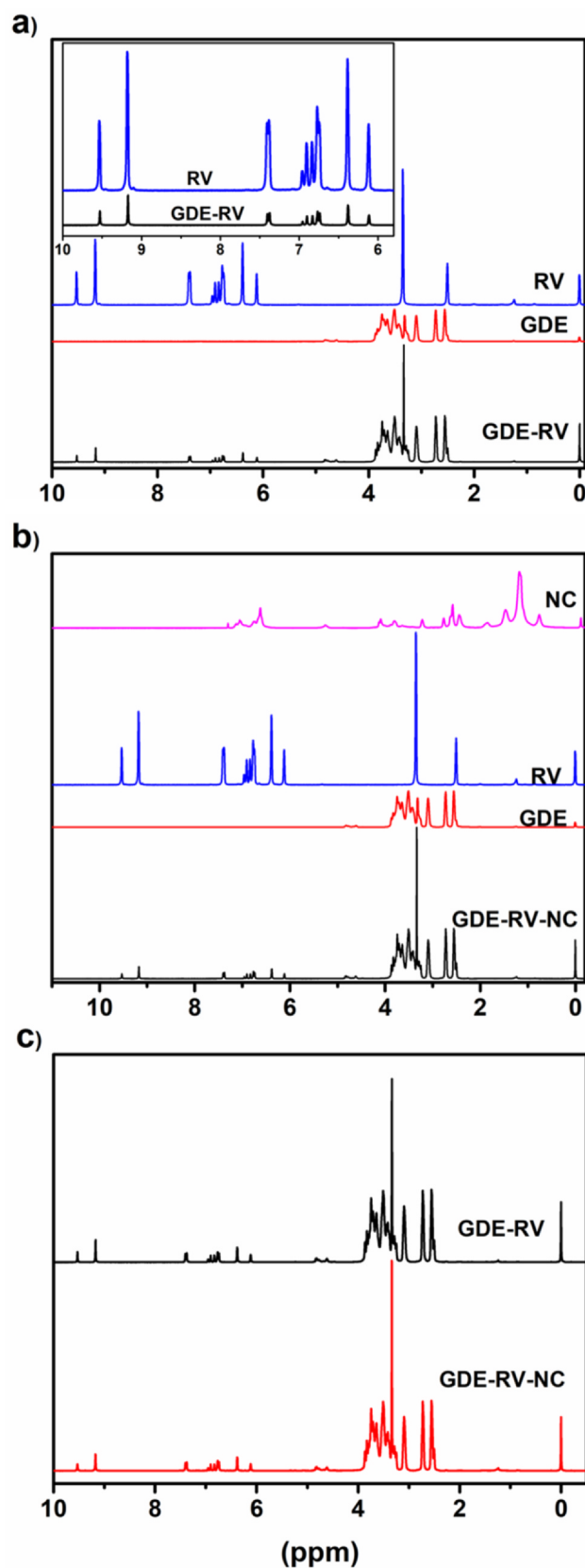


Fig. 5. ^1H NMR spectra of (a) GDE-RV, (b) GDE-RV-NC and (c) GDE-RV and GDE-RV-NC together.

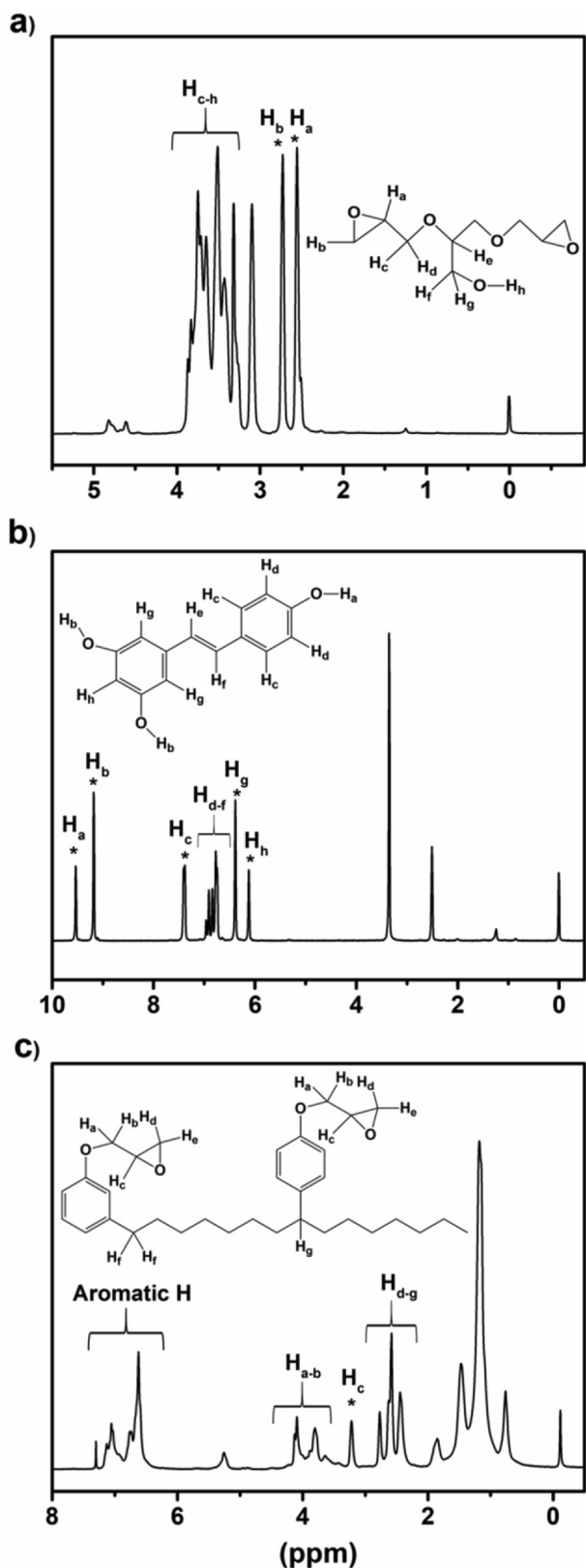


Fig. 6. ^1H NMR spectra of (a) GDE, (b) RV and (c) NC.

demonstrates that GDE is not a single molecule; rather it has an oligomeric structure. A possible cause of the oligomeric nature of GDE could be related to the synthetic methodology employed in the epoxidation of glycerol. A typical epoxidation of an alcohol with epichlorohydrin usually produces oligomers rather than an epoxy

monomer. This observation is also corroborated with higher EEW (146 g/eq) of GDE in comparison with its theoretical EEW (102 g/eq). On the other hand, the exothermic process can be attributed to the presence of impurities as GDE is of technical grade. In contrast, GDE-RV and GDE-RV-NC displayed a shift in the glass transition ($-59\text{ }^\circ\text{C}$) and some small endothermic peaks from $140\text{ }^\circ\text{C}$ to $170\text{ }^\circ\text{C}$. The slightly higher glass transition temperature may be a result of the higher entanglement of GDE with RV and NC. The small endothermic peaks were assigned to the presence of impurities or some unknown reactions. However, it is worth mentioning that these small endothermic peaks are not related to the melting of RV as it happens at around $270\text{ }^\circ\text{C}$ (Fig. 7b).

In summary, based on the NMR results (Figs. 5 & 6), RV has not chemically reacted with GDE during the pre-curing step ($120\text{ }^\circ\text{C}$, 10 min). In addition, since the analysis of the DSC thermographs (Table 2, Fig. 4) suggested that the RV did not chemically react with GDE during the heating ramp, some of the RV may have remained and not covalently bonded to the polymer network in GDE-CA-HA-RV and GDE-CA-HA-RV-NC. The lower reactivity of RV in comparison with CA and HA can be seen in its lower acidity ($\text{pK}_{\text{a}1} = 9.16$, $\text{pK}_{\text{a}2} = 9.77$, $\text{pK}_{\text{a}3} = 10.55$) [55]. The low acidity of RV does not favor the reaction between its hydroxyl groups and the epoxy groups of GDE as it is expected in a polyphenol compound and epoxy resin [56,57]. Furthermore, in terms of stoichiometry, the total amount of CA and HA employed in the formulation can react with 93% of the epoxy groups of GDE, and half of the RV is in excess in relation with GDE. Therefore, considering the above results and the fact that all the epoxy groups were consumed (Fig. 3), it is reasonable to assume that some remaining RV has not covalently bonded to the polymer network. Regarding NC, it is difficult to prove if NC has cross-linked with CA due to its low concentration.

3.3. Thermal and mechanical properties

Glass transition temperatures (T_g) of the bio-based coatings were measured by DSC (Table 3). In addition, the T_g from DMA was calculated as the temperature at which $\text{Tan}\delta$ was the maximum and considered as the T_g values obtained from the DMA experiments (Fig. 8 & Table 3). Both DSC and DMA results showed a characteristic trend of the T_g as the bio-based additives were successively incorporated into the polymer. GDE-CA-0.90 had the highest T_g while GDE-CA-0.73 possessed a slightly lower T_g . The sole incorporation of HA (GDE-CA-HA) caused a further drop in the T_g . However, the subsequent inclusion of RV (GDE-CA-HA-RV) and the further addition of NC (GDE-CA-HA-RV-NC) did not significantly change the T_g . The trend of the T_g values was also corroborated with the storage modulus (E') at $25\text{ }^\circ\text{C}$ of the polymers, which showed that the unmodified samples were stiffer than the modified samples (Table 3).

In addition, we have also assessed the crosslink densities (ν_e) of the bio-based polymers. The ν_e value is calculated from the following equation:

$$\nu_e = \frac{E'}{3RT} \quad (1)$$

where E' is the storage modulus at a specific temperature T in the rubbery state, and R is the universal gas constant [58]. For the calculations, $T = 30\text{ K} + T_g$. Samples GDE-CA-0.90 and GDE-CA-0.73 displayed similar and highest ν_e values. The introduction of HA decreased the ν_e , and the combined incorporation of HA and RV reduced the ν_e even more. Further incorporation of NC did not cause a significant change in the ν_e .

GDE-CA-0.90 had a higher T_g than that of GDE-CA-0.73 but its ν_e was similar to that of GDE-CA-0.73. This result is unusual since GDE-CA-0.90 was expected to have a higher ν_e than that of GDE-CA-0.73 due to the higher concentration of CA in GDE-CA-0.90 that can crosslink with GDE [59]. However, a similar phenomenon was reported in which

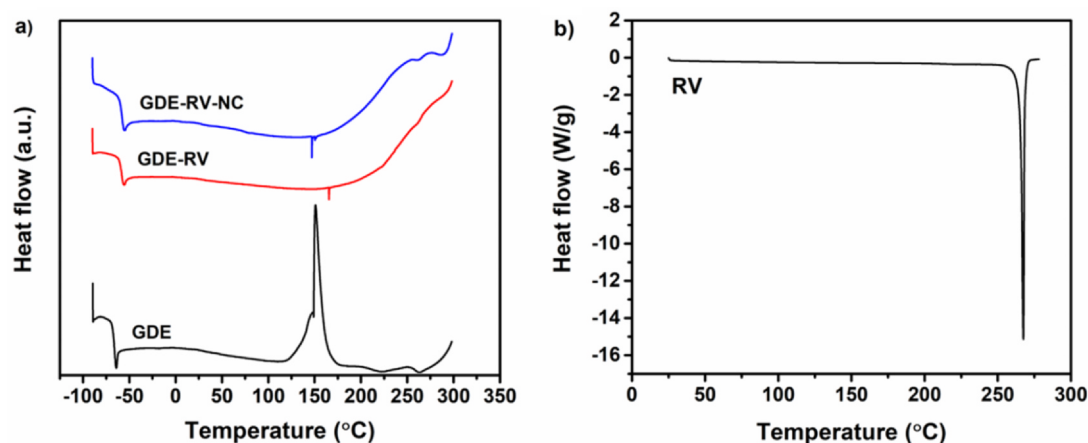


Fig. 7. DSC curves of (a) the precursors GDE-RV and GDE-RV-NC compared with that of GDE and (b) RV.

the T_g of an epoxy polymer increased but its v_c decreased while increasing the concentration of the curing agent [26]. According to the authors, this effect was caused by the intramolecular reactions of the epoxy resin alone. However, the results of Table 3 suggest a possible situation that not all the carboxylic groups of CA in GDE-CA-0.90 have been cross-linked during the polymer reaction. Thus, the incomplete reaction of carboxylic groups may have led to the creation of pendant groups in the polymer network. Although the formation of pendant groups can decrease the T_g [60], it can also have the opposite effect. The presence of pendant groups could also have favored the formation of more entanglements in the polymer and, caused an increase in the T_g [61,62]. Therefore, in comparison with GDE-CA-0.73, an increase in the concentration of CA in GDE-CA-0.90 did not favor an increase in v_c despite that it did favor the formation of pendant groups.

On the other hand, the lower T_g observed in GDE-CA-HA was a result of its low crosslink density. The DSC results (Table 2, Fig. 4) suggest that there was a simultaneous reaction between the bio-based acids (CA and HA) and GDE. Due to the different acidity between CA and HA, it was expected that CA would react with most of the epoxy groups of GDE rather than HA. Therefore, HA was expected to react with the secondary OH groups formed out of the reaction between CA and GDE in the later stage of the curing. However, the DSC results suggest a simultaneous reaction of CA and HA with the resin that may have caused the formation of a branched polymer structure. Thus, the normal reaction between CA and GDE to form a polymer network was hampered by the concurrent reaction between the monofunctional carboxyl acid HA and GDE. In consequence, GDE-CA-HA possessed not only a branched structure but also a low crosslink density (the lower v_c of GDE-CA-HA was proven by the DMA results in Table 3). Therefore, the lower T_g of GDE-CA-HA was ascribed to its low v_c that had a major effect over its branched structure.

Nevertheless, the subsequent incorporation of RV and RV/NC did not significantly change the T_g of the polymer. The T_g values of the modified samples (GDE-CA-HA, GDE-CA-HA-RV and GDE-CA-HA-RV-NC) were quite similar. When comparing GDE-CA-HA and GDE-CA-HA-

RV alone, it was expected that GDE-CA-HA-RV would have higher T_g than that of GDE-CA-HA because of the presence of a rigid additive such as RV. However, this effect was not found because the incorporation of RV decreased the v_c of the polymer (Table 3). Nevertheless, the decrease of the v_c of GDE-CA-HA-RV did not cause a drop in its T_g . Therefore, the results indicate that the lower v_c of GDE-CA-HA-RV might be compensated by the rigidity of RV which has caused its T_g to be similar to that of GDE-CA-HA. On the other hand, GDE-CA-HA-RV and GDE-CA-HA-RV-NC had similar T_g and v_c values, which suggests that NC did not cause any change on these properties. Although NC could have increased the T_g by the creating more entanglements through its aliphatic chains, its low concentration (1%) may have prevented this effect from being perceptible.

The decomposition temperatures of the samples were investigated by TGA. The temperature at 5% mass loss, at 10% mass loss and at the maximum rate of decomposition were calculated and denoted as $T_{d5\%}$, $T_{d10\%}$ and T_{dmax} (°C), respectively (Fig. 9, Table 4). The results show that all the samples possessed very similar $T_{d5\%}$, $T_{d10\%}$ and T_{dmax} . Thus, the bio-based additives did not affect the thermal decomposition properties of the polymers. However, there was an effect on the amount of residue caused by the additives. The percent residues of the unmodified samples (GDE-CA-0.90 and GDE-CA-0.73) and GDE-CA-HA were the lowest among all sample, while GDE-CA-HA-RV and GDE-CA-HA-RV-NC had the highest residue percentages (almost double those of the former group of samples). The highest residue values of the aforementioned samples were ascribed to the presence of RV. This is in agreement with recent reports that polymers containing RV showed higher char yield [37,51]. Therefore, due to its unique molecular structure, RV releases a low concentration of gases when burned and, therefore, conferring a higher char yield.

3.4. Wettability

The water affinity of the samples was assessed by contact angle measurement on coating surfaces and bulk water uptake (Table 5).

Table 3

Glass transition temperature (T_g) and DMA data (storage modulus (E'), crosslink density (v_c) and T_{α}) of the bio-based polymers (values in parentheses represent the standard deviation).

Sample	T_g (°C) (DSC)	T_{α} (°C) (DMA)	E' @ 298.15 K (MPa)	E' @ $T_{\alpha} + 30$ K (MPa)	v_c (mol/m ³)
GDE-CA-0.90	37.3 (± 2.7)	51.1 (± 0.8)	1998 (± 266)	9.2 (± 0.7)	1046 (± 78)
GDE-CA-0.73	30.6 (± 0.9)	45.5 (± 1.2)	2272 (± 172)	10.2 (± 0.4)	1178 (± 39)
GDE-CA-HA	22.6 (± 5.4)	30.8 (± 4.5)	745 (± 482)	6.9 (± 1.3)	824 (± 153)
GDE-CA-HA-RV	26.2 (± 3.1)	34.8 (± 2.0)	606 (± 238)	4.6 (± 0.8)	538 (± 90)
GDE-CA-HA-RV-NC	30.4 (± 1.7)	37.2 (± 2.9)	858 (± 378)	4.2 (± 0.6)	489 (± 70)

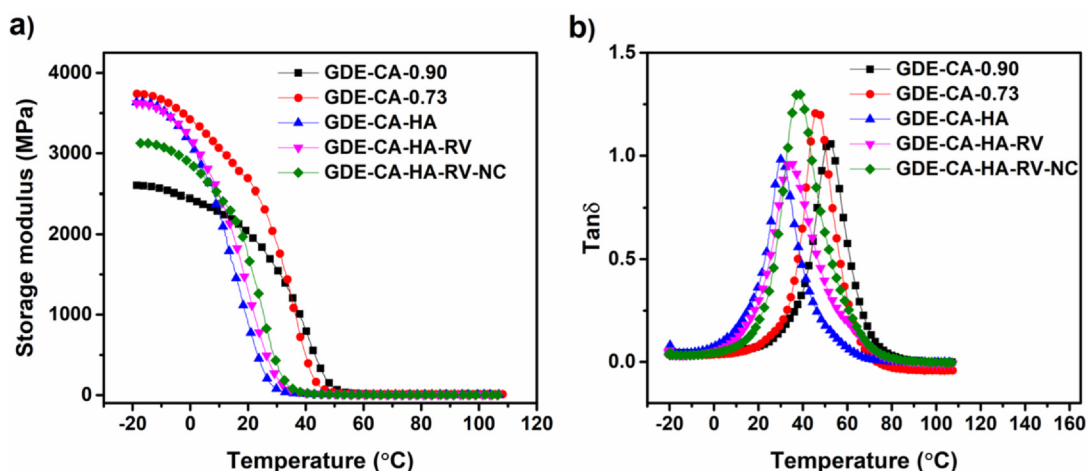


Fig. 8. (a) Storage modulus and (b) $\text{Tan}\delta$ plots of the bio-based polymers.

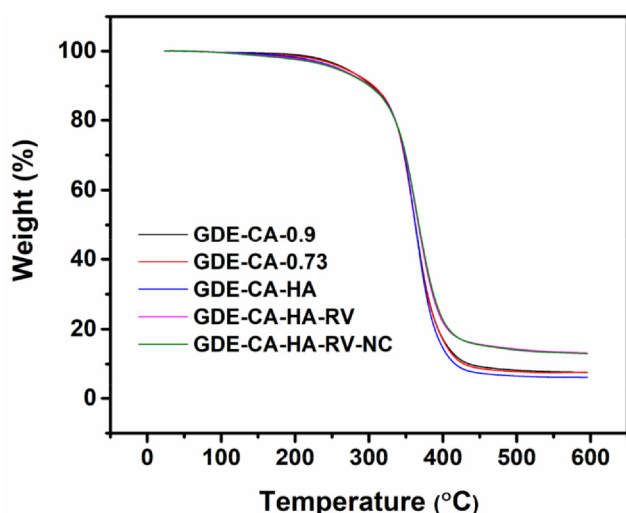


Fig. 9. TGA thermographs of the epoxy cardanol-based coatings.

Based on the wettability properties, the unmodified samples (GDE-CA-0.90 and GDE-CA-0.73) had similar water angles and surface energy. The incorporation of HA and RV did not improve the hydrophobicity. GDE-CA-0.90/0.73 and the modified coatings GDE-CA-HA and GDE-CA-HA-RV displayed similar water contact angles (WCAs) and surface energies. On the other hand, the incorporation of NC caused an increase in the WCA by around 12° and a decrease in the surface energy by 7 mJ/m^2 when compared with the other coatings. The displayed intrinsic hydrophobic properties of NC were in accordance with a previous report [46]. Our results confirm that NC has a better hydrophobic effect over the other bio-based additives (HA and RV). The concentration of the additives did not seem to play a major role in their ability to hydrophobize the coating, as the amount of added NC was the least (1% w/w) as compared with HA (15% w/w) and RV (9% w/w). A possible explanation of the better hydrophobic properties of NC may rely on its

Table 4

Decomposition temperatures and percent residue (values in parentheses represent the standard deviation).

Sample	$T_{d5\%}$ ($^\circ\text{C}$)	$T_{d10\%}$ ($^\circ\text{C}$)	T_{dmax} ($^\circ\text{C}$)	Residue(%)
GDE-CA-0.90	262.7 (± 7.4)	301.6 (± 3.4)	362.1 (± 1.8)	7.50 (± 0.12)
GDE-CA-0.73	268.0 (± 4.0)	306.8 (± 2.1)	362.2 (± 0.3)	7.30 (± 0.36)
GDE-CA-HA	258.5 (± 1.6)	301.5 (± 0.8)	364.2 (± 0.7)	6.04 (± 0.30)
GDE-CA-HA-RV	263.0 (± 5.3)	305.3 (± 3.2)	365.5 (± 1.0)	13.28 (± 0.12)
GDE-CA-HA-RV-NC	261.6 (6.2)	304.1 (3.1)	365.5 (0.7)	12.82 (0.14)

Table 5

Wettability and water uptake data of various formulae (values in parentheses represent the standard deviation).

Sample	WCA ($^\circ$)	Surface energy (mJ/m^2)	Water uptake (%)
GDE-CA-0.90	72.19 (± 2.40)	30.89	33.62 (± 0.91)
GDE-CA-0.73	72.25 (± 3.96)	31.86	32.60 (± 0.91)
GDE-CA-HA	74.96 (± 3.95)	29.87	22.18 (± 0.57)
GDE-CA-HA-RV	75.40 (± 1.90)	28.17	24.15 (± 0.73)
GDE-CA-HA-RV-NC	87.22 (± 1.42)	22.40	23.73 (± 1.08)

molecular structure. As shown in Fig. 1, NC is more flexible, longer and more branched than the other bio-based additives. Thus, it is reasonable to suggest that the molecular structure (length and ramification) of the additive has a great influence on its hydrophobization ability.

The water uptake results were analyzed in terms of the degree of hydrophobicity and crosslink density. It is worth mentioning that water uptake data might be affected by the possible leaching of unreacted soluble components in the formulation. This is an intrinsic issue of this type of experiment. One has to be cautious when comparing the uptake values between formulae that contain precursors with very different solubility.

The unmodified coatings (GDE-CA-0.90 and GDE-CA-0.73) exhibited similar and the highest percent water uptake regardless of the amount of curing agent used. However, the samples modified with the bio-based additives showed similar and lower water uptake values. The unmodified samples had the highest water uptake due to their high degree of hydrophilicity despite of their high degree of crosslink density. Although higher cross-linked polymers are expected to have lower water uptake, the higher hydrophilicity of the GDE and CA drives the diffusion of water into the polymer network. In contrast, the lower water uptake of the samples modified with the bio-based compounds was ascribed to the higher degree of hydrophobicity although they possessed a lower crosslink density. Due to their aliphatic chains and/or benzene groups, the bio-based additives HA, RV and NC are able to

improve the hydrophobicity of the polymers. However, the introduction of the additives caused a decrease in the crosslink density that may favor the diffusion of water molecules. Nevertheless, the hydrophobicity imparted by the bio-based additives played a more dominant role in the water uptake over the crosslink density.

The similar water uptake of the three modified samples can be explained by the similar overall degree of hydrophobicity and crosslink density. For example, GDE-CA-HA had a higher v_e than that of GDE-CA-HA-RV, but both of them had very similar water uptake. This suggests that the hydrophobicity action of RV and HA was more effective than that of HA alone. GDE-CA-HA-RV compensated its lower v_e with a better bulk hydrophobicity granted by RV, which has led to a very similar water uptake as that of GDE-CA-HA. RV seemed to be a better hydrophobizer than HA due to its bigger and more rigid structure. In case of GDE-CA-HA-RV and GDE-CA-HA-RV-NC, their similar water uptake values were the result of their similar v_e values and bulk hydrophobicity. That is, the low concentration of NC did not affect the ultimate bulk hydrophobicity of the polymer network but only the surface hydrophobicity as shown in the WCA and surface energy results. Therefore, the hydrophobic surface effect of NC did not prevent water from coming into the bulk polymer. In summary, the three modified samples had very similar combined effect of crosslink density and hydrophobicity as far as water uptake is concerned.

3.5. Anticorrosion performance

The anticorrosion properties of GDE-CA-0.90, GDE-CA-0.73 and GDE-CA-HA-RV-NC were studied by Tafel analyses (Fig. 10). Table 6 shows the start of corrosion signal, the thicknesses of the samples, the corrosion potential (E_{corr}) and corrosion current (I_{corr}). Materials with high resistance to corrosion are expected to have higher E_{corr} values and lower I_{corr} values. However, after reaching the equilibrium in the seventh day, some samples displayed inconsistent trend for E_{corr} and I_{corr} values, which makes the comparison difficult among them in terms of corrosion resistance (e.g., GDE-CA-0.73 showed a better I_{corr} , but a worse E_{corr} than SS). Nevertheless, the anti-corrosion performance can still be evaluated from the perspective of corrosion delay. The results show that SS without coating started to corrode immediately after being immersed in the electrolyte. In contrast, the corrosion started after several days' immersion in the electrolyte for SS coated with the bio-based polymers. Among the bio-based polymers, GDE-CA-HA-RV-NC delayed the corrosion reaction by 2 more days than GDE-CA-0.90 and GDE-CA-0.73. Since the thickness of the bio-based coatings were quite similar, this result indicates that GDE-CA-HA-RV-NC protected SS

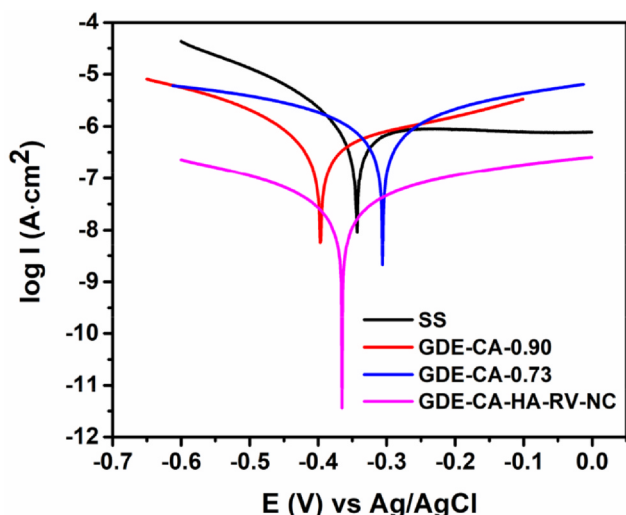


Fig. 10. Typical Tafel curves of the bio-based coatings.

against corrosion better than GDE-CA-0.90 and GDE-CA-0.73 in terms of the corrosion delay. This is in good agreement with the water uptake results (Table 5) in which GDE-CA-HA-RV-NC absorbed less water than GDE-CA-0.90 and GDE-CA-0.73. Overall, the modified coating showed a better corrosion protection than that of the unmodified coating because of its delay effect.

4. Conclusions

New fully bio-based epoxy polymers were prepared using only water as the solvent. The influence of the curing agent concentration and three bio-based additives (HA, RV, NC) on the mechanical and thermal properties, as well as the hydrophobicity and corrosion resistance of the epoxy thermosets were studied. The results show that bio-based additives have been chemically incorporated into the polymer network. Incorporation of the bio-based additives has caused a decrease in the crosslink density, which would eventually affect the mechanical properties of cured polymers. Two main factors were ascribed to this effect. First, HA obstructed the reaction of CA and GDE by reacting with GDE simultaneously. Second, the incorporation of RV and NC has caused a steric impediment on the curing reaction of the small and flexible molecules (GDE, CA and HA) because of their bigger molecular sizes. Nevertheless, the samples modified with the additives were able to absorb a lower amount of water despite of their low crosslink density. The lower water uptake of GDE-CA-HA-RV-NC allowed it to have better anticorrosion performance than GDE-CA-0.90 and GDE-CA-0.73 as shown in its better corrosion delay. Moreover, RV-containing samples were characterized by having higher percentages of chars while NC-containing samples were characterized by their lower surface energy. Finally, it is suggested that the hydrophobic properties of the samples can be improved if the crosslink density is improved. Higher degree of curing can be achieved by various methods such as increasing the curing time/temperature or using catalysts to accelerate specific reactions. We wish that the current work opens an avenue towards fully bio-based environmentally-friendly epoxy coatings for hydrophobic applications.

CRedit authorship contribution statement

Daniel Angel Bellido-Aguilar: Methodology, Investigation, Writing - original draft. **Shunli Zheng:** Writing - review & editing. **Yinjuan Huang:** Investigation, Writing - review & editing. **Ye Sun:** Investigation. **Xianting Zeng:** Conceptualization, Writing - review & editing. **Qichun Zhang:** Conceptualization, Writing - review & editing. **Zhong Chen:** Conceptualization, Writing - review & editing, Supervision.

Declaration of Competing Interest

The authors declare that they have no known competing financial interests or personal relationships that could have appeared to influence the work reported in this paper.

Acknowledgment

We would like to express our gratitude to the Agency for Science, Technology and Research (A*STAR) of Singapore for the funds (SERC 1528000048) provided in this research.

Data availability

The raw/processed data required to reproduce these findings cannot be shared at this time due to technical or time limitations.

Table 6
Corrosion parameters of the bio-based coatings and SS after 7 days of soaking (values in parentheses represent the standard deviation).

Sample	Coating thickness (mm)	Start of Corrosion Signal	E_{corr} (V vs Ag/AgCl)	I_{corr} (A/cm ²) × 10 ⁻⁸
Stainless Steel (SS)	–	Immediately	–0.288 (± 0.05)	109 (± 49.7)
GDE-CA-0.90	2.52 (± 0.078)	~ 5th day	–0.388 (± 0.01)	34.9 (± 23.4)
GDE-CA-0.73	2.54 (± 0.045)	~ 5th day	–0.236 (± 0.03)	55.1 (± 33.9)
GDE-CA-HA-RV-NC	2.66 (± 0.002)	~ 7th day	–0.368 (± 0.00)	3.39 (± 0.23)

References

- J.M. Raquez, M. Deléglise, M.F. Lacrampe, P. Krawczak, Thermosetting (bio)materials derived from renewable resources: A critical review, *Prog. Polym. Sci.* 35 (4) (2010) 487–509.
- H. Nakajima, P. Dijkstra, K. Loos, The Recent Developments in Biobased Polymers toward General and Engineering Applications: Polymers that are Upgraded from Biodegradable Polymers, Analogous to Petroleum-Derived Polymers, and Newly Developed, *Polymers* 9 (10) (2017) 523.
- W. Yuan, S. Ma, S. Wang, Q. Li, B. Wang, X. Xu, K. Huang, J. Chen, S. You, J. Zhu, Synthesis of fully bio-based diepoxymonomer with dicyclo diacetal for high-performance, readily degradable thermosets, *Eur. Polym. J.* 117 (2019) 200–207.
- S.K. Bobade, N.R. Paluvali, S. Mohanty, S.K. Nayak, Bio-Based Thermosetting Resins for Future Generation: A Review, *Polym.-Plastics Technol. Eng.* 55 (17) (2016) 1863–1896.
- M.N. Collins, M. Nechifor, F. Tanasă, M. Zănoagă, A. McLoughlin, M.A. Stróżyk, M. Culebras, C.-A. Teacă, Valorization of lignin in polymer and composite systems for advanced engineering applications – A review, *Int. J. Biol. Macromol.* 131 (2019) 828–849.
- S.G. Tan, W.S. Chow, Biobased Epoxidized Vegetable Oils and Its Greener Epoxy Blends: A Review, *Polym.-Plastics Technol. Eng.* 49 (15) (2010) 1581–1590.
- S. Nameer, D.B. Larsen, J.Ø. Duus, A.E. Daugaard, M. Johansson, Biobased Cationically Polymerizable Epoxy Thermosets from Furan and Fatty Acid Derivatives, *ACS Sustain. Chem. Eng.* 6 (7) (2018) 9442–9450.
- M.D. Garrison, B.G. Harvey, Bio-based hydrophobic epoxy-amine networks derived from renewable terpenoids, *J. Appl. Polym. Sci.* 133 (45) (2016) n/a-n/a.
- R. Auvergne, S. Caillol, G. David, B. Boutevin, J.-P. Pascault, Biobased Thermosetting Epoxy: Present and Future, *Chem. Rev.* 114 (2) (2014) 1082–1115.
- E.A. Baroncini, S. Kumar Yadav, G.R. Palmese, J.F. Stanzione, Recent advances in bio-based epoxy resins and bio-based epoxy curing agents, *J. Appl. Polym. Sci.* 133 (45) (2016) 44103.
- F. Ng, G. Couture, C. Philippe, B. Boutevin, S. Caillol, Bio-Based Aromatic Epoxy Monomers for Thermoset Materials, *Molecules* 22 (1) (2017) 149.
- E. Ramon, C. Guazzo, P.M.G.P. Moreira, A Review of Recent Research on Bio-Based Epoxy Systems for Engineering Applications and Potentialities in the Aviation Sector, *Aerospace* 5 (4) (2018) 110.
- M. Guerfali, I. Ayadi, H.-E. Sassi, A. Belhassen, A. Gargouri, H. Belghith, Biodiesel-derived crude glycerol as alternative feedstock for single cell oil production by the oleaginous yeast *Candida viswanathii* Y-E4, *Ind. Crops Prod.* 145 (2020) 112103.
- A. Schroeder, D.H. Souza, M. Fernandes, E.B. Rodrigues, V. Trevisan, E. Skoronski, Application of glycerol as carbon source for continuous drinking water denitrification using microorganism from natural biomass, *J. Environ. Manage.* 256 (2020) 109964.
- H.W. Tan, A.R. Abdul Aziz, M.K. Aroua, Glycerol production and its applications as a raw material: A review, *Renew. Sustain. Energy Rev.* 27 (2013) 118–127.
- S. Kasetaite, J. Ostrauskaite, V. Grazuleviciene, D. Bridziuviene, R. Budreckiene, E. Rainosal, Biodegradable photocross-linked polymers of glycerol diglycidyl ether and structurally different alcohols, *React. Funct. Polym.* 122 (2018) 42–50.
- S. Kasetaite, J. Ostrauskaite, V. Grazuleviciene, D. Bridziuviene, E. Rainosal, Biodegradable glycerol-based polymeric composites filled with industrial waste materials, *J. Compos. Mater.* 51 (29) (2017) 4029–4039.
- S. Kasetaite, J. Ostrauskaite, V. Grazuleviciene, J. Svediene, D. Bridziuviene, Photocross-linking of glycerol diglycidyl ether with reactive diluents, *Polym. Bull.* 72 (12) (2015) 3191–3208.
- S. Kasetaite, J. Ostrauskaite, V. Grazuleviciene, J. Svediene, D. Bridziuviene, Copolymers of glycerol and propylene glycol diglycidyl ethers with aromatic di-thiols, *J. Appl. Polym. Sci.* 130 (6) (2013) 4367–4374.
- T.N.M.T. Ismail, H.A. Hassan, S. Hirose, Y. Taguchi, T. Hatakeyama, H. Hatakeyama, Synthesis and thermal properties of ester-type crosslinked epoxy resins derived from lignosulfonate and glycerol, *Polym. Int.* 59 (2) (2010) 181–186.
- F.G. Garcia, T.A. Vicente, A.A.A.D. Queiroz, O.Z. Higa, F.J.C. Baratela, Redes epóxi/amina alifáticas com perspectivas para aplicações cardiovasculares. Propriedades biológicas in vitro, *Matéria (Rio de Janeiro)* 21 (2016) 115–128.
- J. Li, L. Fang, W.R. Tait, L. Sun, L. Zhao, L. Qian, Preparation of conductive composite hydrogels from carboxymethyl cellulose and polyaniline with a nontoxic crosslinking agent, *RSC Adv.* 7 (86) (2017) 54823–54828.
- W.J. Wizepman, P. Kofinas, Molecularly imprinted polymer hydrogels displaying isomerically resolved glucose binding, *Biomaterials* 22 (12) (2001) 1485–1491.
- A. Amato, A. Becci, F. Beolchini, Citric acid bioproduction: the technological innovation change, *Crit. Rev. Biotechnol.* 40 (2) (2020) 199–212.
- S.K. Sahoo, V. Khandelwal, G. Manik, Development of completely bio-based epoxy networks derived from epoxidized linseed and castor oil cured with citric acid, *Polym. Adv. Technol.* 29 (7) (2018) 2080–2090.
- S. Ma, D.C. Webster, Naturally Occurring Acids as Cross-Linkers To Yield VOC-Free, High-Performance, Fully Bio-Based, Degradable Thermosets, *Macromolecules* 48 (19) (2015) 7127–7137.
- K. Thiele, N. Eversmann, A. Krombholz, D. Pufky-Heinrich, Bio-Based Epoxy Resins Based on Linseed Oil Cured with Naturally Occurring Acids, *Polymers* 11 (9) (2019) 1409.
- M.F. D'Elia, M. Magni, S.P.M. Trasatti, T.B. Schweizer, M. Niederberger, W. Caseri, Poly(phenylene methylene)-Based Coatings for Corrosion Protection: Replacement of Additives by Use of Copolymers, *Applied Sciences* 9 (17) (2019) 3551.
- A. Adhikari, R. Karpoornath, S. Radha, S.K. Singh, R. Mutthukannan, G. Bharate, M. Vijayan, Corrosion resistant hydrophobic coating using modified conducting polyaniline, *High Perform. Polym.* 30 (2) (2018) 181–191.
- H. Kim, O. Choi, B.S. Jeon, W.-S. Choe, B.-I. Sang, Impact of feedstocks and downstream processing technologies on the economics of caproic acid production in fermentation by *Megasphaera elsdenii* T81, *Bioresour. Technol.* 301 (2020) 122794.
- P. San-Valero, H.N. Abubakar, M.C. Veiga, C. Kennes, Effect of pH, yeast extract and inorganic carbon on chain elongation for hexanoic acid production, *Bioresour. Technol.* 300 (2020) 122659.
- Y. Feng, S. Jie, B.-G. Li, Synthesis of ethylene/vinyl ester copolymers with pendent linear branches via ring-opening metathesis polymerization of fatty acid-derived cyclooctenes, *J. Polym. Sci., Part A: Polym. Chem.* 55 (13) (2017) 2211–2220.
- J.R. Stewart, M.C. Artime, C.A. O'Brian, Resveratrol: A Candidate Nutritional Substance for Prostate Cancer Prevention, *J. Nutr.* 133 (7) (2003) 2440S–2443S.
- F. Zhu, B. Du, J. Li, Recent advance on the antitumor and antioxidant activity of grape seed extracts, *Int. J. Wine Res.* 7 (2015) 63–67.
- M. Zwingelstein, M. Draye, J.-L. Besombes, C. Piot, G. Chatel, Viticultural wood waste as a source of polyphenols of interest: Opportunities and perspectives through conventional and emerging extraction methods, *Waste Manage.* 102 (2020) 782–794.
- Y. Tian, Q. Wang, K. Wang, M. Ke, Y. Hu, L. Shen, Q. Geng, J. Cheng, J. Zhang, From biomass resources to functional materials: A fluorescent thermosetting material based on resveratrol via thiol-ene click chemistry, *Eur. Polym. J.* 123 (2020) 109416.
- L. Shang, X. Zhang, M. Zhang, L. Jin, L. Liu, L. Xiao, M. Li, Y. Ao, A highly active bio-based epoxy resin with multi-functional group: synthesis, characterization, curing and properties, *J. Mater. Sci.* 53 (7) (2018) 5402–5417.
- J.J. Cash, M.C. Davis, M.D. Ford, T.J. Groshens, A.J. Guenther, B.G. Harvey, K.R. Lamison, J.M. Mabry, H.A. Meylemans, J.T. Reams, C.M. Sahagun, High Tg thermosetting resins from resveratrol, *Polym. Chem.* 4 (13) (2013) 3859–3865.
- M. Laskoski, J.S. Clarke, A. Neal, B.G. Harvey, H.L. Ricks-Laskoski, W.J. Hervey, M.N. Daftary, A.R. Shepherd, T.M. Keller, Sustainable High-Temperature Phthalonitrile Resins Derived from Resveratrol and Dihydroresveratrol, *ChemistrySelect* 1 (13) (2016) 3423–3427.
- K. Robinson, C. Mock, D. Liang, Pre-formulation studies of resveratrol, *Drug Dev. Ind. Pharm.* 41 (9) (2015) 1464–1469.
- E. Can, E. Kinaci, G.R. Palmese, Preparation and characterization of novel vinyl ester formulations derived from cardanol, *Eur. Polym. J.* 72 (2015) 129–147.
- A.-S. Mora, R. Tayou, B. Boutevin, G. David, S. Caillol, Synthesis of biobased reactive hydroxyl amines by amination reaction of cardanol-based epoxy monomers, *Eur. Polym. J.* 118 (2019) 429–436.
- A.-S. Mora, M. Decostanzi, G. David, S. Caillol, Cardanol-Based Epoxy Monomers for High Thermal Properties Thermosets, *Eur. J. Lipid Sci. Technol.* 121 (8) (2019) 1800421.
- O. Eksik, A. Maiorana, S. Spinella, A. Krishnamurthy, S. Weiss, R.A. Gross, N. Koratkar, Nanocomposites of a Cashew Nut Shell Derived Epoxy Resin and Graphene Platelets: From Flexible to Tough, *ACS Sustain. Chem. Eng.* 4 (3) (2016) 1715–1721.
- R.S. Gour, V.V. Kodgire, M.V. Badiger, Toughening of epoxy novolac resin using cardanol based flexibilizers, *J. Appl. Polym. Sci.* 133 (16) (2016) 1–9.
- D.A. Bellido-Aguilar, S. Zheng, Y. Huang, X. Zeng, Q. Zhang, Z. Chen, Solvent-Free Synthesis and Hydrophobization of Biobased Epoxy Coatings for Anti-Icing and Anticorrosion Applications, *ACS Sustain. Chem. Eng.* 7 (23) (2019) 19131–19141.
- D.H. Kaelble, Dispersion-Polar Surface Tension Properties of Organic Solids, *J. Adhesion* 2 (2) (1970) 66–81.
- D.K. Owens, R.C. Wendt, Estimation of the surface free energy of polymers, *J. Appl. Polym. Sci.* 13 (8) (1969) 1741–1747.
- W. Rabel, Einige Aspekte der Benetzungstheorie und ihre Anwendung auf die Untersuchung und Veränderung der Oberflächeneigenschaften von Polymeren, *Farbe und Lacke* 77 (10) (1971) 997–1005.
- S.M. Li, T.W. Xu, Z.X. Jia, B.C. Zhong, Y.F. Luo, D.M. Jia, Z. Peng, Preparation and stress-strain behavior of in-situ epoxidized natural rubber/SiO₂ hybrid through a sol-gel method, *eXPRESS Polym. Lett.* 12 (2) (2018) 180–185.
- Y. Tian, Q. Wang, L. Shen, Z. Cui, L. Kou, J. Cheng, J. Zhang, A renewable

- resveratrol-based epoxy resin with high Tg, excellent mechanical properties and low flammability, *Chem. Eng. J.* 383 (2020) 123124.
- [52] D.A. Bellido-Aguilar, S. Zheng, X. Zhan, Y. Huang, X. Zhao, X. Zeng, P.K. Pallathadka, Q. Zhang, Z. Chen, Effect of a fluoroalkyl-functional curing agent on the wettability, thermal and mechanical properties of hydrophobic biobased epoxy coatings, *Surf. Coat. Technol.* 362 (2019) 274–281.
- [53] J. Søtoft-Jensen, F. Hansen, 15 - New Chemical and Biochemical Hurdles, in: D.-W. Sun (Ed.), *Emerging Technologies for Food Processing*, Academic Press, London, 2005, pp. 387–416.
- [54] B.-Y. Wang, N. Zhang, Z.-Y. Li, Q.-L. Lang, B.-H. Yan, Y. Liu, Y. Zhang, Selective Separation of Acetic and Hexanoic Acids across Polymer Inclusion Membrane with Ionic Liquids as Carrier, *Int. J. Mol. Sci.* 20 (16) (2019) 3915.
- [55] L. Zimányi, S. Thekkan, B. Eckert, A.R. Condren, O. Dmitrenko, L.R. Kuhn, I.V. Alabugin, J. Saltiel, Determination of the pKa Values of trans-Resveratrol, a Triphenolic Stilbene, by Singular Value Decomposition Comparison with Theory, *J. Phys. Chem. A* 124 (31) (2020) 6294–6302.
- [56] Y.-O. Kim, J. Cho, H. Yeo, B.W. Lee, B.J. Moon, Y.-M. Ha, Y.R. Jo, Y.C. Jung, Flame Retardant Epoxy Derived from Tannic Acid as Biobased Hardener, *ACS Sustain. Chem. Eng.* 7 (4) (2019) 3858–3865.
- [57] M. Korey, G.P. Mendis, J.P. Youngblood, J.A. Howarter, Tannic acid: A sustainable crosslinking agent for high glass transition epoxy materials, *J. Polym. Sci., Part A: Polym. Chem.* 56 (13) (2018) 1468–1480.
- [58] J. Wan, B. Gan, C. Li, J. Molina-Aldareguia, E.N. Kalali, X. Wang, D.-Y. Wang, A sustainable, eugenol-derived epoxy resin with high biobased content, modulus, hardness and low flammability: Synthesis, curing kinetics and structure–property relationship, *Chem. Eng. J.* 284 (2016) 1080–1093.
- [59] A.P. Gupta, S. Ahmad, A. Dev, Development of Novel Bio-Based Soybean Oil Epoxy Resins as a Function of Hardener Stoichiometry, *Polym.-Plastics Technol. Eng.* 49 (7) (2010) 657–661.
- [60] N.L. Dias Filho, C.X. Cardoso, H.A.D. Aquino, Relationships between the curing conditions and some mechanical properties of hybrid thermosetting materials, *J. Braz. Chem. Soc.* 17 (2006) 935–943.
- [61] D.T. Turner, Glass transition elevation by polymer entanglements, *Polymer* 19 (7) (1978) 789–796.
- [62] Y. Ma, Y. Liu, T. Yu, W. Lai, Z. Ge, Z. Jiang, Structure–property relationship of nitramino oxetane polymers: a computational study on the effect of pendant chains, *RSC Adv.* 9 (6) (2019) 3120–3127.